Journal Name



ARTICLE TYPE

Cite this: DOI: 10.1039/xxxxxxxxxx

Magnetic order and enhanced exchange in the quasi-one-dimensional molecule-based antiferromagnet $Cu(NO_3)_2(pyz)_3^{\dagger}$

Benjamin M. Huddart,* a Jamie Brambleby, b Tom Lancaster, a Paul A. Goddard, b Fan Xiao, c,d Stephen J. Blundell, e Francis L. Pratt, f John Singleton, g Piero Macchi, c Rebecca Scatena, c Alyssa M. Barton, h and Jamie L. Manson,* h

Received Date Accepted Date

DOI: 10.1039/xxxxxxxxxx

www.rsc.org/journalname

The quasi-one-dimensional molecule-based antiferromagnet $\mathrm{Cu(NO_3)_2(pyz)_3}$ has an intrachain coupling J=13.7(1) K and exhibits a state of long-range magnetic order below $T_\mathrm{N}=0.105(1)$ K. The ratio of interchain to intrachain coupling is estimated to be $|J'/J|=3.3\times10^{-3}$, demonstrating a high degree of isolation for the Cu chains.

Recent progress in the field of molecular magnetism has shown the clear potential for gaining control over the structural building blocks of molecular materials in order to engineer desirable magnetic properties. Bridging ligands such as pyrazine (=pyz= $C_4H_4N_2$) facilitate exchange interactions between transtion metal ions and allow for the construction of polymeric networks whose primary exchange occurs along one, two or three dimensions $^{1-3}$. The manipulation of these building blocks, combined with further ingredients such as counterions 4,5 and additional ligands 6 , enables the synthesis of materials with a wide range of magnetic properties. Furthermore, such systems

act as experimental realizations of simple and well-studied model systems, such as the one-dimensional⁷ and two-dimensional⁸ S = 1/2 quantum Heisenberg antiferromagnet.

The molecule-based antiferromagnet $\operatorname{Cu(NO_3)_2(pyz)}$ (1) represents a highly-ideal experimental realization of the one-dimensional quantum Heisenberg antiferromagnet (1DQHAFM)⁹. Antiferromagnetic coupling between $\operatorname{Cu^{2+}}$ ions is facilitated by pyz ligands [see Fig.1(a)] with an exchange constant J=10.5 K determined from measurements of magnetic susceptibility, specific heat and neutron scattering⁹. Weak interchain coupling J' results in a state of 3D long range magnetic order at T=0.107 K, which was detected using muon-spin relaxation 10 . These measurements give an estimate $|J'/J|=4.4\times 10^{-3}$ for the ratio of interchain to intrachain coupling 10 .

In this paper, we report the magnetic properties of the Heisenberg antiferromagnetic chain system Cu(NO₃)₂(pyz)₃ (2) ¹¹. Like 1, 2 comprises Heisenberg $S = 1/2 \text{ Cu}^{2+}$ ions connected via pyrazine ligands to form a chain along the a-axis [Fig. 1(b)]. Different from 1, each metal centre has two further transcoordinated non-bridging pyrazine ligands extending perpendicular to the chains, keeping them well separated [Fig. 1(b)]. This results in a regular octahedral environment for the Cu^{2+} ions in 2, which has a much higher degree of symmetry than the distorted octahedral environment for Cu²⁺ in 1 [Fig. 1(a)]. For 2, we obtain an intrachain coupling of J = 13.7(1) K (30% larger than in 1) from measurements of magnetic susceptibility and pulsed-field magnetization and we argue that different local environments for the Cu²⁺ ions is the main factor responsible for this higher intrachain coupling. Muon-spin spectroscopy reveals a state of long range magnetic order below $T_{\rm N}$ =0.105(1) K. The ratio of interchain to interchain coupling is lower than that obtained for 2, suggesting that this system is an even more successful realization of a 1DQHAFM.

^a Centre for Materials Physics, Durham University, South Road, Durham DH1 3LE, United Kingdom. E-mail: benjamin.m.huddart@durham.ac.uk

b Department of Physics, University of Warwick, Gibbet Hill Road, Coventry, CV4 7AL, United Kingdom.

^c Department of Chemistry and Biochemistry, University of Bern, Freiestrasse 3, Bern, 3012. Switzerland.

 $[^]d$ Laboratory for Neutron Scattering and Imaging, Paul Scherrer Institut, CH-5232 Villigen PSI, Switzerland.

 $[^]e$ Department of Physics, Clarendon Laboratory, University of Oxford, Parks Road, Oxford OX1 3PU, United Kingdom.

 $[^]f$ ISIS Pulsed Muon Facility, STFC Rutherford Appleton Laboratory, Chilton, Didcot, OX11 0QX, United Kingdom.

[§] National High Magnetic Field Laboratory, Los Alamos National Laboratory, MS-E536, Los Alamos, New Mexico 87545, United States.

h Department of Chemistry and Biochemistry, Eastern Washington University, Cheney, Washington 99004. United States. E-mail: imanson@ewu.edu

 $[\]dagger$ Electronic Supplementary Information (ESI) available: CIF for Cu(NO_3)_2(pyz)_3 at 173 K. Experimental details for magnetic susceptibility, pulsed-field magnetization and muon-spin spectroscopy measurements. See DOI: 10.1039/b000000x/

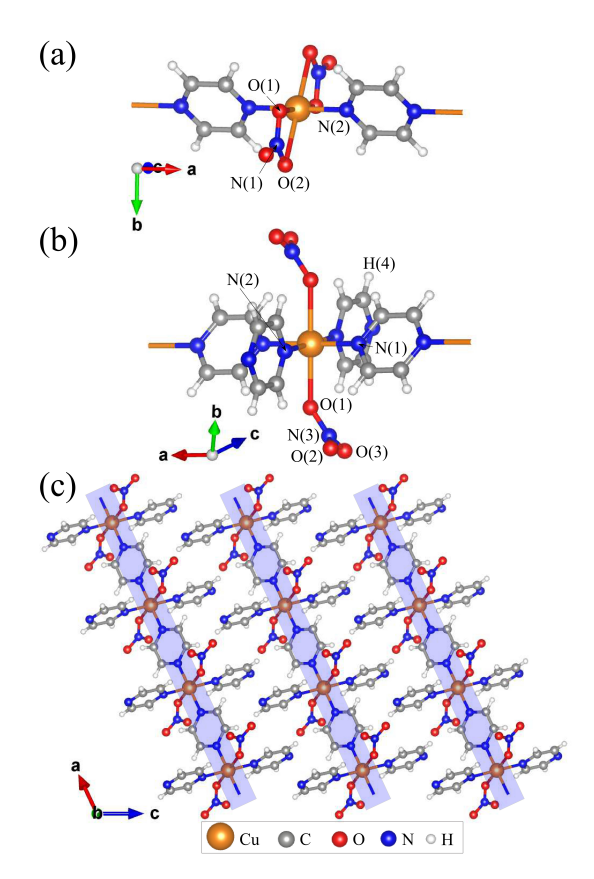


Fig. 1 Local environments of the Cu^{2+} ions in (a) 1 and (b) 2. (c) Structure of 2 demonstrating the packing of chains.

We prepared deep blue rods of 2 following the procedure previously described by Parkin et al. 11§. We re-determined the X-ray crystal structure of as it is relevant to our interpretation of its magnetic properties (see ESI[†]). Different to 1, which contains four oxygen donor atoms (from chelated nitrate ligands) and two N-donor atoms from pyz, 2 contains two oxygen donor atoms from coordinated NO3 - ligands and four N-donor atoms belonging to pyz [Cu-N(1) = 2.069(2) and Cu-N(3) = 2.020(2) Å]. The Cu²⁺ ion in 2 is elongated due to Jahn-Teller distortion along the O-Cu-O axis [Cu-O(1) = 2.400(2) Å]. Importantly, this places the magnetic $d_{x^2-y^2}$ orbital in the CuN_4 plane such that it can interact with two other Cu²⁺ ions along the chain through pyz-bonds. The resulting structure is that of a polymeric linear chain [Fig. 1(c)] which propagates along the crystallographic *a*-axis. Successive chains stagger along the *c*-direction and pack to form pseudo two-dimensional sheets in the ab-plane [Fig. 1(c)]. Supramolecular interactions within these sheets are weak whereas H(4) forms a bifurcated interaction with the two non-coordinated oxygen atoms from NO₃-, O(2) and O(3), at distances of 2.579 Å and 2.530 Å, respectively. As a result of these weak interchain interactions we anticipate negligible magnetic coupling between them as well.

The measured molar susceptibility, χ_{mol} , of 2 [Figure 2(a)]

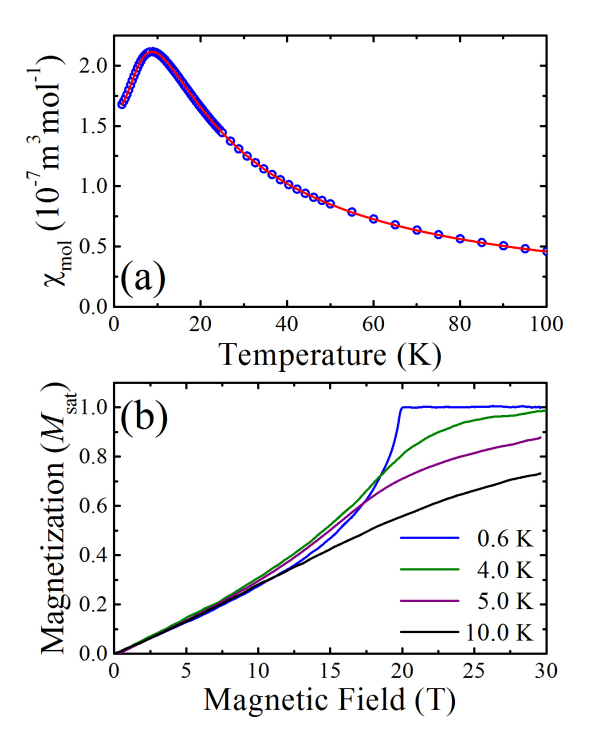


Fig. 2 (a) Molar susceptibility $(\chi_{\rm mol})$ vs. temperature for a polycrystalline sample of ${\rm Cu(NO_3)_2(pyz)_3}$ (circles) shows a broad maximum at 9 K. The data have been fitted to a model of spin-1/2 Heisenberg moments connected in a 1D chain with nearest-neighbour exchange J^{13} (line), yielding g=2.04 and J=13.7 K. **(b)** Magnetization in units of the saturation magnetization $(M_{\rm sat})$ vs magnetic field provided by a short-pulse magnet. Down sweeps of the magnetic field at various temperatures are shown. The data at the lowest temperature are typical of highly isolated S=1/2 antiferromagnetic chains.

shows a broad maximum at 9 K indicative of the individual copper moments becoming correlated along the chains and the onset of low-dimensional behaviour below this temperature. Motivated by the structural analysis, the data are fitted to a model of S=1/2 Heisenberg spins connected in a 1D chain with a single nearest-neighbour interaction J^{13} . The resultant fitted parameters are g=2.04(1) and J=13.7(1) K. A Curie-Weiss analysis of the inverse susceptibility data for temperatures above 100 K returned fitted values g=2.03(1) and an antiferromagnetic Curie-Weiss temperature $|\theta_{\rm CW}|=5.4(5)$ K, which is consistent with the energy scale and nature of the intrachain Heisenberg exchange constant.

Pulsed-field magnetization measurements up to 60 T (rise time to full field \sim 10 ms) were carried out at the National High Magnetic Field Laboratory in Los Alamos. The magnetization measured at various temperatures is shown in Figure 2(b) as a fraction of the saturated value. The concave rise observed at the lowest temperature and the sharp change in gradient at saturation is characteristic of highly isolated S=1/2 antiferromagnetic chains, where, for the ideal system, $\mathrm{d}M/\mathrm{d}B$ is known to diverge at the saturation field 14 . As the temperature increases the magnetization exhibits a more gradual approach to saturation.

The structural, susceptibility and magnetization data all imply that the interchain interactions are orders of magnitude smaller than the intrachain exchange (J). In this case, the low-

 $[\]S$ Further increasing the amount of pyrazine in the chemical reaction yields square plates of $[Cu(NO_3)(pyz)_2]NO_3 \cdot H_2O$ recently reported by some of us ¹².

temperature value of J can be estimated from the saturation field $B_{\rm C}^{\ 4}$ via the expression $g\mu_{\rm B}B_{\rm C}=2J$. From the T=0.6 K magnetization data it is found that $B_{\rm C}=19.9(1)$ T and so, using the g-factor determined from the Curie-Weiss fit, the exchange energy is found to be 13.6(1) K, in agreement with the result of fitting the magnetic susceptibility.

Implanted muons are very sensitive to small magnetic fields and were therefore used to probe the low-temperature magnetic behaviour. Zero-field muon-spin relaxation (ZF μ^+ SR) measurements were made on a polycrystalline sample using the low temperature facility (LTF) spectrometer at the Swiss Muon Source. Example μ^+ SR spectra are shown in Figure 3. For T<0.105 K we can resolve oscillations at a single frequency in the asymmetry, A(t), characteristic of quasistatic long range magnetic order (LRO) at one magnetically distinct muon site. We note that, in an earlier work on 1, oscillations in the μ^+ SR spectra were observed at two distinct frequencies 10 ; the additional pyz branches in 2 may block muons from occupying one of the candidate muon sites. We fit the spectra to the functional form

$$A(t) = A_1 e^{-\lambda_1 t} + A_2 e^{-\lambda_2 t} \cos(2\pi v t + \phi) + A_{\text{bg}}, \tag{1}$$

where the components with amplitudes A_1 and A_2 , due to muons stopping in the sample, have relaxation rates λ_1 and λ_2 respectively and the component with amplitude A_2 oscillates with a frequency v. $A_{\rm bg}$ is the constant background asymmetry due to muons in the sample holder or those with their spins aligned parallel to the internal field. Above T = 0.105 K the spectra change shape and we instead fit the data to the sum of a Gaussian and an exponential relaxation. The temperature dependence of v is shown in Figure 3. The oscillation frequency vis related to the magnitude of the magnetic field at the muon site through $v = \gamma_{\mu} B/2\pi$ where γ_{μ} is the muon gyromagnetic ratio (= $2\pi \times 135.5 \text{MHz T}^{-1}$) and serves as effective order parameter for the system. A fit to the phenomenological function $v(T) = v(0)[1 - (T/T_N)^{\alpha}]^{\beta}$ with $\alpha = 3$ (fixed) yields v(0) =1.59(1) MHz, $\beta = 0.12(2)$ and $T_N = 0.105(1)$ K [see Figure 3(a)]. A critical exponent $\beta = 0.18(5)$ was previously obtained for 1, which is conistent with 2D Ising or 2D XY models ¹⁰. The value of β obtained for **2** is even smaller and closer to that of a 2D Ising model, for which one expects $\beta = 1/8$. This might suggest that the fluctuations that destroy the LRO are two dimensional, most likely occuring along the chains and along the strongest exchange pathway between chains.

Periodic DFT Calculations were carried out using the software CRYSTAL14¹⁵. The functional B3LYP was used with basis set 86-411G(41d)¹⁶ for the Cu and pob–TZVP¹⁷ for all the other atoms. Gas-phase DFT calculations on a dimeric unit were carried out with Gaussian09¹⁸ using again the B3LYP functional and the basis set 6-311G(2d,2p). We have calculated the exchange couplings J using both periodic DFT and gas phase DFT on a single dimer and find J=14.88 K and J=11.49 K respectively. Our calculations indicate antiferromagnetic coupling between Cu spins and show reasonable agreement with the values of J obtained experimentally. These values are larger than the coupling constants J=10.70 K and J=11.02 K obtained for $\bf 1$ using periodic DFT and

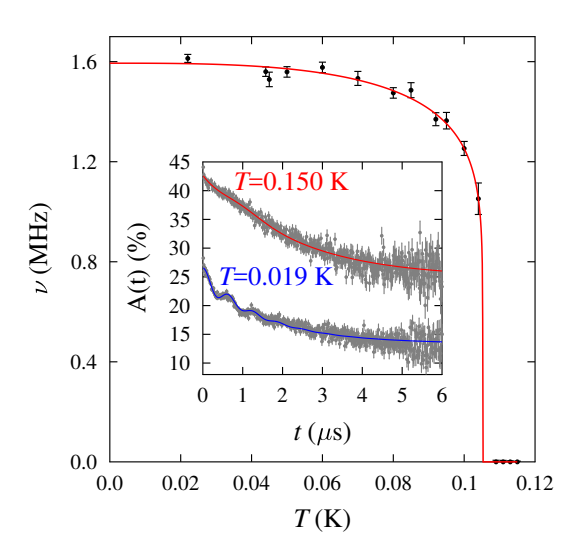


Fig. 3 Temperature dependence of (a) the frequency and (b) the relaxation parameter λ_2 in equation 1. Inset: example $\mu^+ SR$ spectra for $Cu(NO_3)_2(pyz)_3$ measured above and below the magnetic ordering temperature.

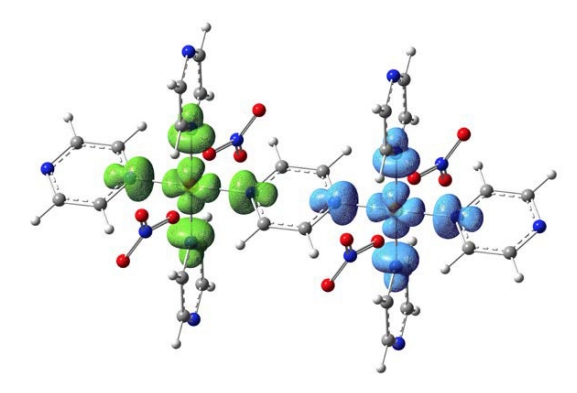


Fig. 4 Spin density distribution through pyrazine ligand calculated using density functional theory.

a dimer fragment approach repectively ¹², supporting the experimentally observed trend. The calculated spin density distribution through the pyrazine ligand is shown in Figure 4. The largest part of the spin density is located at the copper atoms, with some delocalisation to the adjacent N atoms.

The combination of our measurements of the intrachain coupling J (from magnetic susceptibility) and the ordering temperature $T_{\rm N}$ (from $\mu^+ {\rm SR}$) allows us to estimate the interchain coupling J' through

$$|J'|/k_{\rm B} = \frac{T_{\rm N}}{4c\sqrt{\ln\left(\frac{\lambda|J|}{k_{\rm B}T_{\rm N}}\right) + \frac{1}{2}\ln\ln\left(\frac{\lambda|J|}{k_{\rm B}T_{\rm N}}\right)}},\tag{2}$$

where $\lambda=2.6$ and $c=0.223^{19}$. Substituting $|J|/k_{\rm B}=13.7$ K and $T_{\rm N}=0.105(1)$ K we obtain $|J'|/k_{\rm B}=0.045$ K and $|J'/J|=3.3\times 10^{-3}$. These values are very similar to those obtained for ${\bf 1}^{10}$. Furthermore, we can obtain an estimate of the magnetic moment of ${\rm Cu}^{2+}$ in this system through $m\approx 1.017\left|J'/J\right|^{1/2}2^0$ and obtain $m\approx 0.059~\mu_{\rm B}$. The moment is very small, highlighting the effect

of quantum fluctuations in suppressing the ordered moment in this low-dimensional system.

In both 1 and 2, a Jahn-Teller distortion places lobes of the Cu $d_{x^2-y^2}$ orbitals along the Cu-N bonds. The primary exchange pathway between Cu²⁺ ions is through the bridging pyz ligands along a 1D chain in both compounds and results in them having similar magnetic properties. However, the precise environments of the Cu^{2+} ions in the two cases are quite different. In 1 the $d_{x^2-y^2}$ orbital lies in the plane containing the Cu-N bonds and the two shorter Cu-O(1) bonds. The Cu ion forms bonds to both two of the O atoms in the nitrate ligand and the inherent rigidity of the nitrate group results in an O(1)-Cu-O(2) angle of 57°, far from the ideal 90° for octahedral symmetry [see Fig.1(a)]. The Cu²⁺ ion therefore sits in a highly distorted octahedral environment. In **2**, the $d_{x^2-y^2}$ orbital lies in the plane containing four Cu-N bonds with the Cu-O bonds lying perpendicular to this plane, completing the octahedral coordination [see Fig.1(b)]. This results in a higher symmetry environment for Cu^{2+} in 2 than in 1.

In superexchange processes the exchange coupling $J \approx$ $\sum |H_{fi}|^2/\Delta E$ depends on the orbital overlap H_{fi} between the orbitals involved in virtual hopping processes and the difference ΔE between energy levels on the magnetic ion and the non-magnetic intermediary. Given that in both 1 and 2 superexchange occurs through magnetic $d_{x^2-v^2}$ orbitals which can interact with other Cu²⁺ ions through pyz bonds, we expect the orbital overlap to be similar, explaining the similarity in values of J. However, J also depends on higher order virtual processes which may be affected by the different environments for Cu in the two cases. We expect the lower symmetry environment of Cu in 1 to result in splittings of the d orbitals. In particular, we expect the repulsion between O(2) and the $d_{x^2-y^2}$ (which would be smaller if O(2) was occupying the ideal octahedral position) to raise the energy of electrons in the $d_{x^2-v^2}$ orbital and thus increase ΔE . Processes like these could explain the fact that J is larger in 1 than in 2.

In **1** and **2** the angles between pyz and the plane containing the $d_{x^2-y^2}$ orbitals are similar (51° and 55° respectively) and we find that J in **1** is smaller despite the tilt angle being closer to the theoetically ideal value of 45° which would be expect to maximize π -overlap ²¹. This is consistent with a study on **1** and the quasi-2D/3D antiferromagnet [Cu(NO₃)(pyz)₂]NO₃·H₂O (3) ¹² where bond ellipticity profiles of the related compounds **1** and **3** were taken to rule out a mechanism driven by the π -overlap between the d_{yz} and d_{xy} orbitals of Cu and the π orbitals at the pyrazine in favour of a mechanism based on σ -exchange only.

The quasi-two-dimensional Cu-based antiferromagnet **3** is structurally similar to **1** and **2**, with pyz ligands again allowing coupling between Cu^{2+} ions 12 . Despite the dimeric unit of **3** and its associated spin density 12 being nearly identical to that for **2**, the lack of staggering between chains (present for **1** and **2**) results in significant overlap between trans-coordinated pyz orbitals and the Cu^{2+} ions in adjacent chains. This additional exchange pathway results in a quasi-two-dimensional system with a reduced exchange constant J = 7.3 K.

In conclusion, the spin-1/2 chain compound $\text{Cu}(\text{NO}_3)_2(\text{pyz})_3$ exhibits a larger intrachain coupling J=13.7 K and a lower magnetic ordering temperature $T_{\text{N}}=0.105$ K than $\text{Cu}(\text{NO}_3)_2(\text{pyz})$,

making it a more successful realization of a 1DQHAFM. Its success as a quasi-one-dimensional system is likely due a more symmetrical environment for the Cu^{2+} ion that enhances J and the presence of non-bridging pyz branches that assist to maintain effective chain isolation.

We are grateful to the Swiss Muon Source for the provision of beamtime. We thank Chris Baines for experimental assistance. We thank EPSRC for financial support. B Huddart thanks STFC for support via a studentship. The work at EWU was supported by the U.S. National Science Foundation (NSF) under grant no. DMR-1703003. Data will be made available via Durham Collections.

Conflicts of interest

There are no conflicts to declare.

Notes and references

- J. L. Manson, M. M. Conner, J. A. Schlueter, T. Lancaster, M. L. B. Stephen J. Blundell, F. L. Pratt, T. Papageorgiou, A. D. Bianchi, J. Wosnitza and M.-H. Whangbo, *Chem Commun.*, 2006, 4894

 –4896.
- 2 J. L. Manson, M. L. Warter, J. A. Schlueter, T. Lancaster, A. J. Steele, S. J. Blundell, F. L. Pratt, J. Singleton, R. D. McDonald, C. Lee, M.-H. Whangbo and A. Plonczak, *Angewandte Chemie International Edition*, 50, 1573–1576.
- 3 J. L. Manson, J. A. Schlueter, K. A. Funk, H. I. Southerland, B. Twamley, T. Lancaster, S. J. Blundell, P. J. Baker, F. L. Pratt, J. Singleton, R. D. McDonald, P. A. Goddard, P. Sengupta, C. D. Batista, L. Ding, C. Lee, M.-H. Whangbo, I. Franke, S. Cox, C. Baines and D. Trial, *Journal of the American Chemical Society*, 2009, 131, 6733–6747.
- 4 P. A. Goddard, J. Singleton, P. Sengupta, R. D. McDonald, T. Lancaster, S. J. Blundell, F. L. Pratt, S. Cox, N. Harrison, J. L. Manson, H. I. Southerland and J. A. Schlueter, New J. Phys., 2008, 10, 083025.
- 5 A. J. Steele, T. Lancaster, S. J. Blundell, P. J. Baker, F. L. Pratt, C. Baines, M. M. Conner, H. I. Southerland, J. L. Manson and J. A. Schlueter, *Phys. Rev. B*, 2011, 84, 064412.
- 6 P. A. Goddard, J. Singleton, I. Franke, J. S. Möller, T. Lancaster, A. J. Steele, C. V. Topping, S. J. Blundell, F. L. Pratt, C. Baines, J. Bendix, R. D. McDonald, J. Brambleby, M. R. Lees, S. H. Lapidus, P. W. Stephens, B. W. Twamley, M. M. Conner, K. Funk, J. F. Corbey, H. E. Tran, J. A. Schlueter and J. L. Manson, *Phys. Rev. B*, 2016, 93, 094430.
- 7 G. Müller, H. Thomas, H. Beck and J. C. Bonner, *Phys. Rev. B*, 1981, **24**, 1429–1467.
- 8 E. Manousakis, Rev. Mod. Phys., 1991, 63, 1-62.
- P. R. Hammar, M. B. Stone, D. H. Reich, C. Broholm, P. J. Gibson, M. M. Turnbull,
 C. P. Landee and M. Oshikawa, *Phys. Rev. B*, 1999, 59, 1008–1015.
- T. Lancaster, S. J. Blundell, M. L. Brooks, P. J. Baker, F. L. Pratt, J. L. Manson,
 C. P. Landee and C. Baines, *Phys. Rev. B*, 2006, **73**, 020410.
- 11 T. Otieno, A. M. Gipson and S. Parkin, J. Chem. Crystallogr., 2002, 32, 81-85.
- 12 L. H. R. Dos Santos, A. Lanza, A. M. Barton, J. Brambleby, W. J. A. Blackmore, P. A. Goddard, F. Xiao, R. C. Williams, T. Lancaster, F. L. Pratt, S. J. Blundell, J. Singleton, J. L. Manson and P. Macchi, J. Am. Chem. Soc., 2016, 138, 2280–2291
- 13 D. C. Johnston, R. K. Kremer, M. Troyer, X. Wang, A. Klümper, S. L. Bud'ko, A. F. Panchula and P. C. Canfield, *Phys. Rev. B*, 2000, 61, 9558–9606.
- 14 J. C. Bonner and M. E. Fisher, Phys. Rev., 1964, 135, A640–A658.
- 15 R. Dovesi, R. Orlando, A. Erba, C. M. Zicovich-Wilson, B. Civalleri, S. Casassa, L. Maschio, M. Ferrabone, M. De La Pierre, P. D'Arco, Y. Noël, M. CausàÂã, M. Rérat and B. Kirtman, *International Journal of Quantum Chemistry*, 114, 1287–1317.
- 16 K. Doll and N. Harrison, Chemical Physics Letters, 2000, 317, 282 289.
- 17 M. F. Peintinger, D. V. Oliveira and T. Bredow, Journal of Computational Chemistry, 34, 451–459.
- M. J. Frisch, G. W. Trucks, H. B. Schlegel, G. E. Scuseria, M. A. Robb, J. R. Cheeseman, G. Scalmani, V. Barone, B. Mennucci, G. A. Petersson, H. Nakatsuji, M. Caricato, X. Li, H. P. Hratchian, A. F. Izmaylov, J. Bloino, G. Zheng, J. L. Sonnenberg, M. Hada, M. Ehara, K. Toyota, R. Fukuda, J. Hasegawa, M. Ishida, T. Nakajima, Y. Honda, O. Kitao, H. Nakai, T. Vreven, J. A. Montgomery, Jr., J. E. Peralta, F. Ogliaro, M. Bearpark, J. J. Heyd, E. Brothers, K. N. Kudin, V. N. Staroverov, R. Kobayashi, J. Normand, K. Raghavachari, A. Rendell, J. C. Burant, S. S. Iyengar, J. Tomasi, M. Cossi, N. Rega, J. M. Millam, M. Klene, J. E. Knox, J. B. Cross, V. Bakken, C. Adamo, J. Jaramillo, R. Gomperts, R. E. Stratmann, O. Yazyev, A. J. Austin, R. Cammi, C. Pomelli, J. W. Ochterski, R. L. Martin, K. Morokuma, V. G. Zakrzewski, G. A. Voth, P. Salvador, J. J. Dannenberg, S. Dapprich, A. D. Daniels, A. Farkas, J. B. Foresman, J. V. Ortiz, J. Cioslowski and D. J. Fox, Gaussian 09, Gaussian Inc. Wallingford CT 2009.
- C. Yasuda, S. Todo, K. Hukushima, F. Alet, M. Keller, M. Troyer and H. Takayama, Phys. Rev. Lett., 2005, 94, 217201.
- 20 H. J. Schulz, Phys. Rev. Lett., 1996, 77, 2790-2793.

21	H. W. Richardson and W. E. Hatfield, <i>Journal of the American Chemical Society</i> , 1976, 98 , 835–839.